

Design, Simulation, Fabrication and Evaluation of a Textile PIFA for Wearable IoT Application

Azadeh Ahmadihaji¹, Hadi Aliakbarian²,
Nordiana Mohamad Saaid³, and Ping Jack Soh^{3,4}

ABSTRACT: The ever increasing use of body-worn systems in the Internet of Things application needs better antenna subsystem designs compatible with its requirements. Several challenges limiting the performance of a body-worn system, from materials, and environmental conditions to the effects of on body application and its hazards are discussed. As a test case, a flexible textile Planar Inverted-F antenna is presented and discussed. The choice of this topology is due to its simplicity in design and fabrication, relatively broad bandwidth and the presence of a rear ground plane, which minimizes the impacts of the human body on the antenna performance. It is designed on a felt substrate, whereas Aaronia-shield conductive textile is utilized as its conductive parts (radiator, shorting wall and ground plane). The antenna performance is studied in two cases, first in free space and then in bent conditions in the close proximity to the human body. The influence of the relative humidity on the textile antenna performance is also investigated numerically. Simulated and measured results indicated good agreements. Finally, the proposed antenna is integrated with a transceiver module and evaluated on the body in practice. Its wireless link quality is assessed in an indoor laboratory.

Keywords: Wearable Antenna, Textile Antenna, Planar Inverted-F Antenna, Humidity Effect, Specific Absorption Rate, Wireless Link Evaluation

DOI: 10.37936/ecti-cit.2021153.241779

Article history: received July 26, 2020; revised December 5, 2020; accepted January 16, 2021; available online October 29, 2021

1. INTRODUCTION

Services and systems related to the Internet of things (IoT) have attracted increasing attention in recent years. They potentially provide solutions in applications such as smart agriculture, smart homes, shopping systems, smart grids, health-care, health monitoring, and so on [1-2], as illustrated in Figure 1. One of the most promising applications of such a system in recent years is elderly care. The elderly population has constantly been increasing in most developed countries, thus increasing the costs drastically for providing long-term health care and well-being

services. This has motivated researchers to explore possible implementations of wearable wireless health-monitoring systems (WWHMs), which integrate various wearable or implantable sensors to communicate physiological parameters wirelessly to health practitioners. The data can be communicated to a wearable central node prior to transmission to a medical cloud-based system for further processing.

The need for the development of IoT services has triggered the industry to propose wireless technology solution and standards. Bluetooth Low Energy (BLE) for instance, has been one of the pioneering

^{1,2}The authors are with The Wireless Terminals Measurement Lab, K.N.Toosi University of Technology, Iran., E-mail: azadeh.ahmadihaji.1@ens.etsmtl.ca and aliakbarian@kntu.ac.ir

^{3,4}The authors are with Advanced Communication Engineering (ACE) CoE, Faculty of Electronic Engineering Technology, Universiti Malaysia Perlis, Pauh Putra Campus, 02600 Arau, Perlis, Malaysia., E-mail: dianams@unimap.edu.my and pjsoh@unimap.edu.my

⁴The author is with Centre for Wireless Communications (CWC), University of Oulu, Erkki Koiso Kanttilan Katu 3, 90570 Oulu, Finland., E-mail: pingjack.soh@oulu.fi

technologies in enabling the combination IoT technology and the wearability of the device. On the other hand, making an IoT system body-worn is challenging and necessitates a better physical layer design that is compatible with the specific requirements of IoT. Antennas and RF front end sections are one of the challenging sections of the physical layer, which profoundly affects a wearable system's performance. Various factors may limit the performance of a body-worn system, from materials, and environmental conditions to the effect of on body operation.



Fig.1: IoT Services Across User's Daily Activities.

Wearable antenna is a vital interface for wireless communication between on-body sensors and off-body devices in wearable IoT, which can be integrated into clothing to ensure comfort [3]. Since wearable antennas play an integral role in IoT systems, they have drawn considerable interest in literature [2], [4-8]. Depending on the type of application and services these systems operate in, various wearable antennas with different features have been proposed. However, as a general requirement, they should be lightweight, low-profile, easy to manufacture and cost-effective. Furthermore, they must feature simple and fast installation while being easy to maintain. These antennas are used in proximity of the human body, and their operation under various curvatures, situations, and in different climates have been investigated. This requires the assessment of parameters such as specific absorption rate (SAR), bending performance, and moisture absorption.

Since more than a decade ago, researches have introduced various wearable antennas, which have been designed based on either conventional planar dipoles antennas [4], planar monopoles [5], planar inverted-Fs (PIFAs) [6], [7], and microstrip patch antennas [8]. These antenna types are preferred due to their low cost and ease of fabrication. In this paper, a PIFA is chosen due to its small electrical size, simple design, and popularity. The ground plane on its rear, despite being relatively small, enables its operation near the human body with minimized effects. This article is aimed at exploring wearable antennas in general and PIFA specifically, the different challenges they face such as SAR, effects of the body, hu-

midity, or moisture impacts. Next, the PIFA is prototyped, measured, and compared with simulations. The design and parametric analysis of the antenna is performed using the time domain solver in CST Microwave StudioTM. The initial antenna design is designed based on the PIFA in [9], prior to further optimization in terms of reflection coefficient and radiation pattern in flat and bent states are simulated for operation in the ISM band with satisfactory robustness. The influence of humidity and the human body (arm) on antenna performance are also investigated. Besides this, measurements of the antenna performance are performed using a Vector Analyzer Network (Rohde & Schwarz ZVL-13). Due to the limited number of past literature assessing link quality as an end to an antenna work, a communication link evaluation with a base station using the proposed PIFA is performed. The major contribution of this work is the followings:

1. Design, simulation, and fabrication of a compact PIFA with a wide impedance bandwidth using felt substrate.
2. Evaluation of the impact of bending, the human body, and humidity on the antenna performance.
3. The antenna sensitivity measurement via the integration of the antenna with a transceiver module, and evaluation of the wireless link.

The following section will first present a brief review on body-worn antennas available in the literature. This is followed by a literature review on several wearable antennas for IoT applications and a discussion of their challenges. Section 4 will introduce the design of the proposed wearable PIFA. In Section 5, the sensitivity analysis of the PIFA under different situations is studied. They include when the antenna is operated in close proximity to the human body or when it is bent. Then, the assessment of moisture content and its impacts on the performance of the antenna is investigated in Section 6. In Section 7, the PIFA fabrication and measurements, both its radiation patterns and its reflection coefficients are presented. The antenna is finally integrated with an nRF24L01 wireless module working in the 2.4 GHz band and worn on-body to evaluate the wireless link's performance in Section 8. Finally, this paper is concluded in Section 9.

2. BODY-WORN ANTENNAS: A BRIEF REVIEW

Wireless Body Area Networks (WBAN) require a wide bandwidth to guarantee continuous operation [10]. On the other hand, the human body, as a lossy medium, degrades antenna performance significantly. Therefore, it is crucial to design wearable antennas such that they could compensate for inaccuracies caused by the human body. For example, a wider bandwidth (usually more than 5 %) is consid-

Table 1: A Comparison between Some Wearable Antennas.

Ref	Year	Ant. Type (number)	Dielectric and metallic Material	Dimensions (mm)	Radiation Efficiency	Max Directivity (dBi)	BW
[17]	2019	CPW-Fed Slot Antenna(1)	Felt ($\epsilon_r = 1.36$)	15X17X1	48% @5.8GHz	(measured gain) 4.85 dBi @ 5.8GHz	100MHz
[18]	2018	Dual-band patch antenna with a dedicated varactor-loaded module (2)	C-Foam PF-4 Cuming Microwave ($\epsilon_r = 1.06$)	About 60x55x4 (considering snap-on button)	75% @ lower band	(measured gain) 3.1 dB @ 2.44GHz	About 100MHz @ lower band
					88.3% @ upper band	(measured gain) 8.3 dB @ 5.8 GHz	About 150MHz @ upper band
[21]	2017	E-shaped microstrip monopole antenna with an EBG Structure (3)	denim ($\epsilon_r = 1.7$)	46x46x2.4	-	7.8 dBi	660 MHz
[19]	2016	Patch antenna (4)	Felt($\epsilon_r = 1.3$)	100x100x3.34	38% @n=0 mode	2.0 dB (gain) @n=0 mode	(measured bandwidth) 157 MHz @ n=0 mode
					45% @n=+1 mode	3.9dB (gain) @n=+1 mode	(measured bandwidth) 119 @ n=+1 mode
[12]	2015	Magneto-Electric Dipole antenna (5)	Felt ($\epsilon_r = 1.37$)	100x100x3	Above 50% lower band and 60% upper band	Better than 4.7	490 MHz lower band (2.45GHz band)
[16]	2014	A patch Antenna with an AMC plane (6)	Felt ($\epsilon_r = 1.2$)	100x100x3.84	above 40%	2.89 dB @ lower band	About 400MHz @ lower band
						4.398 dB @ upper band	About 700MHz @ upper band
[13]	2014	Slot* (7)	denim ($\epsilon_r = 1.7$) ShieldIt	73.78x67x0.95	flat@ 2.5GHz:89%	flat@ 2.5GHz:4.65dB	-
					Convex 35mm@ 91%	Convex 35mm@ 3.45dB	
[20]	2014	PIFA (8)	$\epsilon_r = 1$	30x33x4	On phantom less than 50%	-	On phantom about 340 MHz
					On human model less than 30%		human body about 350 MHz
[15]	2013	PIFA (9)	Fleece as substrate($\epsilon_r = 1.17$) denim host $\epsilon_r = 1.7$	70x30x4 (with ground)	About 60%	5dB	650 MHz
[9]	2011	PIFA* (10)	Fleece ($\epsilon_r = 1.17$)	50x19x6	PCPTF 76.6%	PCPTF 1.51 dB	PCPTF 1115 MHz
					ShieldIt 77.2%	ShieldIt 1.53 dB	ShieldIt 1280 MHz
[14]	2007	Microstrip Patch (11)	Aramid ($\epsilon_r = 1.75$)	44x42x1.67 Ant (66mm with GND)	70% on body	8	Slightly over 100 MHz

ered advantageous for these antennas [11]. Furthermore, the performance of textile antennas is mainly affected by choice of the substrate, its thickness, and the geometry of the patch. The resonant frequency of the antenna, its gain, and efficiency can be improved by choosing the substrates with lower permittivity [11]. The geometry of the antenna should be chosen such that the antenna remains compact and lightweight while maintaining satisfactory efficiencies and gain. Low profile antenna is preferable to ensure

low fabrication cost in mass production and the least interference with the user's comfort.

Various researches have been performed in designing efficient wearable antennas, and they are summarized in Table 1. The researchers in [12] introduced a dipole featuring two U-shaped slots made fully using textiles, except for the feeding connector. The performance of this design is found to be robust against bending when assessed on the body. Next, the work in [13] proposed a slotted antenna design,

which was then evaluated under a flat and bent condition in free space. Denim fabric was used as the substrate, with an L-shaped slot integrated in the ground plane of this antenna structure. Meanwhile, in [14], a rectangular patch antenna was proposed for integration into a fire fighter's jacket. For PIFAs, a PIFA structure is introduced in [9] to achieve a large bandwidth and avoid detuning caused by the human body. Next, researchers in [15] have investigated the effects of embroidered conductive patterns on a PIFA's performance. Besides, an artificial magnetic conductor (AMC) plane is used as a ground plane in [16] to reduce the backward radiation.

Among the works presented in Table 1, it is noticed that the slot antenna in [17] and patch antennas in [18] and [19] are incapable of providing large bandwidths to potentially alleviate any additional detuning caused by the human body. Furthermore, the final antenna in [19] is relatively large. The size of the PIFA in [20] is suited for wearable applications, but its efficiency when simulated on-body and on-phantom is less than 50%. Similar to the work presented in [18] and [19], the patch antenna of [14] has a relatively limited bandwidth of about 100 MHz. Considering its radiation pattern and high backward radiation, the slot antenna proposed in [13] is unsuitable for on-body use. Meanwhile, the antennas in [12] and [16] perform almost the same in terms of the backward radiation and bandwidth, and their sizes are electrically large. From literature, PIFA structures presented in [15] and [9] are good choices for on-body application considering structure simplicity, bandwidth and gain. The latter is selected as the basis of this design due to its smaller size, better efficiency and larger bandwidth.

3. CHALLENGES OF BODY-WORN ANTENNAS

Antenna design for wearable applications is challenging, considering different factors such as the flexible materials that are used. As wearable antennas are used in proximity to the human body, its operation under various curvatures, environments, and in different climates has been investigated. This investigation requires the assessment of parameters such as specific absorption rate (SAR), bending performance, and moisture absorption to be accounted for in the design process. Besides, wearable antennas should be lightweight, thin, and enable fabrication simplicity to ensure cost-effectiveness. In the following part of this section, five of these issues are discussed.

3.1 Material and Methods

The first issue regarding body-worn systems is the material chosen for both the substrate and conducting part of the antenna. The subsection discusses the critical aspects in selection of materials for the antenna's development.

3.1.1 Dielectric Substrate

The choice of substrate for wearable antennas is very important to guarantee consistent performance. Textile fabrics are mainly low in permittivity, ε , and this parameter is usually expressed as follows:

$$\varepsilon = \varepsilon_0 \varepsilon_r = \varepsilon_0 (\varepsilon_r' - j\varepsilon_r'') \quad (1)$$

In (1), ε_0 is the permittivity of vacuum, which is equal to $8.854 \times 10^{-12} \text{ F/m}$, ε_r is relative permittivity, which consists of two parts: its real part is ε_r' which is also called dielectric constant, although it is not constant in all frequencies, and its imaginary part is ε_r'' . The ratio of ε_r'' to ε_r' is called the loss tangent, $\tan \delta = \varepsilon_r''/\varepsilon_r'$. The relatively low permittivity of between 1 and 2 in textiles reduces the surface wave losses and increases the antenna impedance bandwidth (BW). One of the important factors determining the dielectric properties of textile substrates is the moisture content of the materials [22]. Meanwhile, the thickness of the substrate also influences the antenna bandwidth. This can be explained in terms of the antenna quality factor, Q , as summarized in equation (2), as follows:

$$BW \sim 1/Q \quad (2)$$

The Q coefficient is influenced by four factors, including space wave losses (Q_{rad}), the ohmic conduction losses (Q_c), the dielectric losses (Q_d) and surface waves losses (Q_{sw}) as specified in equation (3). For thin substrates ($h \ll \lambda_0$), Q_{rad} is generally the dominant factor and is inversely proportional to the substrate thickness.

Therefore, increase in the substrate height results in lower Q factor (Q_t) and thus, a wider antenna bandwidth [22].

$$\frac{1}{Q_t} = \frac{1}{Q_{rad}} + \frac{1}{Q_c} + \frac{1}{Q_{sw}} + \frac{1}{Q_d} \quad (3)$$

3.1.2 Conductive Textiles

The fabrics used for designing textile antennas must be high in conductivity to minimize electrical losses. This factor, when it is less than 10^3 S/m , is capable of affecting antenna efficiency. Besides, fabrics must have enough flexibility for body-worn applications and be stretchable so that the final antenna structure can be deformed to support wearable applications. An interesting investigation in choosing the type of conductive textile was performed in [23], where a simple patch antenna has been designed and fabricated using four different conducting fabrics e.g. Flectron, Shieldit, Zelt, and Taffeta. Results indicated that Taffeta fabric performed the best relative to the other three fabrics due to its high conductivity. It was also shown that these conductive fabrics could be applied for antennas, similar to copper sheets [23].

Besides the aforementioned aspects, the fabrication techniques have a dominant role in determining the wearable antenna's final cost and speed of production. A dual-band textile monopole antenna with a synthetic fabric as its dielectric substrate for IOT application has been presented in [24]. The antenna components were assembled using an adhesive sheet by ironing with and without steam. Applying steam can cause higher compaction of the antenna material, increasing its substrate permittivity or lowering its radiating parts' conductivity, which in turn leads to a higher frequency shift [24]. It is also shown that conductive fabric orientation does not have any impact on antenna performance. Seven prototypes of these antennas were fabricated by two manufacturing methods, lamination, and embroidering. Embroidering reduces production costs, which is suitable for mass production. However, in this method, the direction of stitches towards the feed line and the number of stitches may affect antenna performance. An antenna with a lower number of stitches and stitch direction parallel with the feed line showed a higher match based on simulation results. Integration of the antenna into clothing also does not influence antenna behavior [24].

3.2 Moisture

Textile antennas which have been integrated into garments will be used in various environmental conditions. One of the most important parameters that can significantly affect the performance of wearable antennas is the humidity. Humidity changes the dielectric properties of the substrate. This is due to the high permittivity of water ($\epsilon_r = 78$ at 25°C and 2.45 GHz), and its ease in seeping through the mainly air-filled cavities of the textile materials [25].

its Moisture Regain (MR), which is defined as the level of moisture presence in a material (at 20°C and 65% relative humidity) in comparison to its dry state [25]. Increasing the relative humidity (rH) increases relative permittivity, consequently shifting the resonant frequency downwards. Moreover, increasing rH causes more losses in the material, which leads to a wider band operation and smaller resonance peak. Materials with a higher MR have a higher tendency to be influenced by changes in humidity [25]. The effect of relative humidity on a patch antenna with five different substrate materials is summarized in Table 2.

These materials have been referred to as:

- NAT 1: Jeans, a woven 100% cotton fabric
- NAT 2: A woven fabric consisting of flax yarn as a wrap and cotton yarn as weft
- NATSYN: A woven fabric, including 50% cotton and 50% polyamide (nylon)
- SYN: A fleece fabric consisting of polyethylene terephthalate (PET)
- FOAM: A polyurethane-based flexible foam

Table 2: Properties of the substrate materials [25].

	MR(%)	ϵ_r	Tan δ	h(mm)
NAT 1	7.33	1.71	0.020	1.090
NAT 2	8.02	1.70	0.020	0.858
NATSYN	5.68	1.60	0.020	0.400
SYN	0.95	1.15	0.000	2.060
FOAM	1.99	1.50	0.001	3.500

Three prototypes were built for each substrate and all 15 prototypes were placed at least for 24 hours in a test cabinet, at a temperature of 23°C and a rH of 10, 20, 30, 40, 50, 60, 70, 80 and 90% [25]. To minimize the influence of the moisture absorption on the antenna resonant frequency, a synthetic fabric with low MR was chosen by [25].

3.3 Antenna Performance Under Deformations

The use of flexible materials for comfort purposes in garments potentially causes physical deformations to wearable antennas such as bending. Bending the antenna changes its electrical characteristics and radiation properties. Besides that, physical properties such as thickness may result in the variation of bulk permittivity, which consequently affects antenna bandwidth and resonant frequency. An investigation on the effects of bending on a PIFA in [26] indicated that the bending in the x -direction over a hypothetical cylinder deteriorated its reflection coefficient (S_{11}) and bandwidth at the higher frequencies. On the contrary, bending in the y -direction did not affect the antenna bandwidth significantly in the upper band. However, in the lower band and with more extreme bending, the antenna performance suffered from degradations. The radiating edge of the PIFA is the main resonance generating mechanism and influences its behavior under bending. The radiating edge is only bent at the x -direction, rendering mechanical changes at the y -direction is ineffective at changing the surface current flowing on the radiator. Gain variation is more intuitive when the antenna is bent in the y -direction. Also, it is found that bending along the radiating edge using the smallest cylinder radius resulted in the worst antenna performance in terms of bandwidth, reflection coefficient, and gain [26].

3.4 Specific Absorption Rate (SAR) of Wearable Antennas

The microwave radiation may potentially enhance temperature in human cells, which then may give rise to dielectric heating. The main safety parameter for the operation of wearable antennas operating in the vicinity of the human body is the SAR (in W/kg). It is a parameter that measures the rate of energy ab-

sorption by the human tissues when exposed to RF electromagnetic fields. This parameter can be calculated by the following equation:

$$SAR = \frac{P}{\rho} = \frac{\sigma |E|^2}{\rho} \quad (4)$$

where P is the power absorbed per mass of tissue (W), ρ is the mass density (Kg/m³), σ is the electrical conductivity (S/m), and $|E|$ is the root-mean-square electric field strength (in V/m). SAR is typically expressed as average power absorbed by a small volume of tissues, which is either 1g or 10g [27].

One of the main concern on the use of wearable antennas is maintaining its SAR value under international standards' limitation. The work in [28] presented a wearable triband dipole antenna with low SAR for IoT applications. This antenna with a semi-omnidirectional pattern comprises two symmetrical E-shaped patches backed by a rectangular patch with L-shaped cuts on a denim substrate. The rectangular patch with L-shaped cuts increased the antenna bandwidth and the operating frequency band [28]. However, the influence of bending on antenna performance was not significant. There is a good agreement between the antenna's on-body and off-body measured reflection coefficient when the wearable antenna was placed on different parts of the human body, including the chest, arm, wrist, and leg. However, antenna gain and efficiency were considerably affected [28]. For an input power of up to 100 mW, the average SAR (10g) peak value was 1.71 W/Kg (at 5.75 GHz), which meets International Electrotechnical Commission (IEC) standards. Increasing input power will lead to a significant increase in SAR values.

The use of conductive textiles with lower conductivities causes higher antenna SAR. It is also dependent on the distance between the antenna and the body. Selecting an appropriate antenna topology and ground plane size can ensure that the antenna operates below the safety limit. In general, antennas with higher backward radiation have higher SAR values [27].

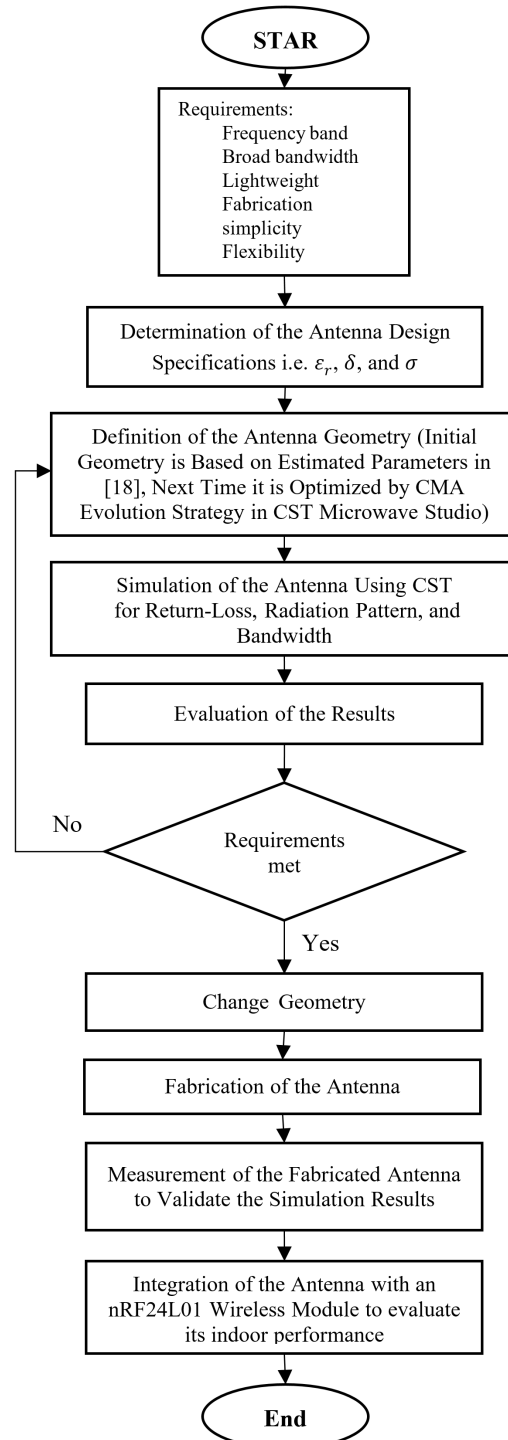


Fig.2: Methodology flowchart.

3.5 Effects of the Human Body

Placement and operation of any radiating structure in the vicinity of the human body will certainly affect parameters such as the reflection coefficient, bandwidth, gain, efficiency, and radiation characteristics, due to the coupling and absorption by the human body. This is due to the human body, which acts as a dielectric and lossy medium. In [29] an investiga-

tion using three circular wearable antennas operating in close proximity to the human body indicated that their resonant frequencies shifted upwards. This is due to the reduction of effective capacitance between the patch and ground plane, which are in series. In addition, intuitively, operation near a lossy medium leads to the decrease in the antenna's quality factor, and thus a marginal increase in impedance bandwidth can be observed. Besides that, the operation of wearable antennas in the vicinity of the human body will reduce efficiency and gain [29]. The efficiency of small antennas can be improved by using metamaterial and fractal technology. Moreover, the operating range of an antenna can be increased while maintaining size compactness by the fractal slot structures. This was proposed for IoT applications in frequencies ranging from 0.5 GHz to 4 GHz in [30]. The gain and directivity of this patch antenna with split-ring resonators (SRR), has been enhanced by 2.5 dB than the patch antenna without SRR [30].

Furthermore, when a wearable antenna is placed on the body, a limitation in the direction of radiation is expected. To overcome this, the wearable antennas can be integrated with the reconfigurable feature. A polarization reconfigurable wearable antenna with a total dimension of $70 \times 70 \times 4 \text{ mm}^3$ for IoT applications is presented in [31]. Four PIN diodes control the truncations on the radiating patch and provide three polarization modes, including LHCP, RHCP, and LP. These three modes have a front-to-back ratio of above 23 dB. The bandwidth of this antenna covers the overall 2.4 GHz ISM band [31].

4. DESIGN OF TEXTILE PIFA

Figure. 2 illustrates the methodology used in this research. The proposed PIFA structure is consists of a radiator, a shorting wall, a ground plane, a substrate, and a feeding probe. This antenna is designed based on [9] with a focus on achieving a broad bandwidth. Its ground plane prevents severe detuning when operating in close proximity to the human body. An empirical formula in [32] is used for the calculation. This formula, shown in equation (5), is suitable for antennas with dimensions of $S_h + R_w + R_L < \lambda$. In (5) W_f is the width of the feed. f_v and f_h are respectively the vertical and horizontal distance of a 50Ω SMA port from the edge of the shorting plate. Other dimensions are depicted in Figure. 3. In equation (5) f_c is central frequency, which is 2.45GHz in this work, c is the speed of light, R_W and R_L are the width and length of the radiator, respectively, and W_W is shorting wall width. The ground plane has a length and width of $G_L \times G_W$, and the substrate has a height of S_h .

$$f_c = \frac{c}{3R_w + 5.6R_L + 3.7S_h - 3W_f - 4.3\sqrt{f_h^2 + f_v^2}} \quad (5)$$

This equation may only provide an initial estimate for the PIFA dimensions and is limited in terms of dimensional accuracy. Thus, the calculation of the initial design in [9] is performed using equation (5). Upon simulating the initial antenna using dimensions provided in [9], the antenna is optimized using CMA Evolution Strategy in the simulation software. In this simulation algorithm, some variables are considered for antenna dimensions, and they are altered to obtain resonance at the desired frequency of 2.45 GHz. The estimated radiator size before and after optimization is approximated to be $19 \times 21 \text{ mm}^2$ and $19 \times 20 \text{ mm}^2$, respectively.

A conventional PIFA shown in Figure.3 is chosen as the design. ShieldIt conductive textile, which is 0.17 mm thick, is used as conductive components of the antenna (radiator, shorting wall, and ground plane). A 4 mm-thick felt with a relative permittivity of $\epsilon_r=1.45$ and $\tan \delta = 0.044$ is used as the substrate. For simulation simplicity, the conductive textile is assumed as a metal (with a conductivity, $\sigma = 5.9 \times 10^7 \text{ S/m}$). All antenna dimensions are summarized in Table 3.

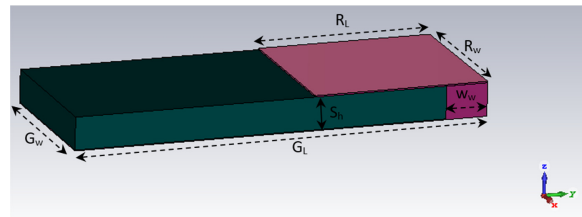


Fig.3: The proposed PIFA structure [9].

Table 3: Dimensions of the proposed PIFA [9].

Parameter	W_w	f_v	f_h	R_w	R_L	G_w	G_L
Size (mm)	5.0	9.5	8.5	19	21	19	50

5. SENSITIVITY ANALYSIS

The most common factor affecting antenna performance is the impact of the proximity of the human body. The human body is an electrically lossy medium, with each tissue having dissimilar complex dielectric constants. This lossy medium affects the reflection coefficient and bandwidth of the antenna. To analyze this effect, the antenna is assumed to be located on an arm model. Simulations were performed using CST Microwave Studio (MWS) software. A four-layered arm model which is consist of the skin, fat, muscle, and bone (listed from the outer to inner layer) is used in this analysis. The permittivity, conductivity, and density of each material is extracted from the software's material library. The thickness of each layer is listed in Table 4, and the model is illustrated in Figure 6(a). To represent the gap between

antenna and human body, the proposed antenna is located 15 mm away from the human tissue when it is under evaluation. Due to the use of the open boundary condition beneath the tissue model in the simulation, the depth of the tissue model is assumed to be infinite, which is a good approximation.

The relationship between the injected signal into the antenna and the reflected signal is described as a reflection coefficient. The reflection of the injected signal happens due to the impedance mismatch. An ideal impedance matching will result in a minimum reflection coefficient. Due to the interaction between the human model and antenna, the reflection coefficient changes depending on the proximity of the human body. The simulated antenna reflection coefficients (S11) of the cases with and without the tissues in flat states are compared in Figure 4. It can be seen that the presence of the tissues resulted in an extra resonance at 2.26 GHz, besides causing the 2.45 GHz center frequency to be shifted upwards to 2.62 GHz. There is also an increase in the -10 dB impedance bandwidth of the antenna by approximately 50 MHz, from 700 MHz in free space to 750 MHz in proximity of the body. The radiation patterns of the antenna in free space and in proximity of the human body are compared in Figure 5. It is noticed that due to the presence of the human body, the radiation pattern is directed away from the body.

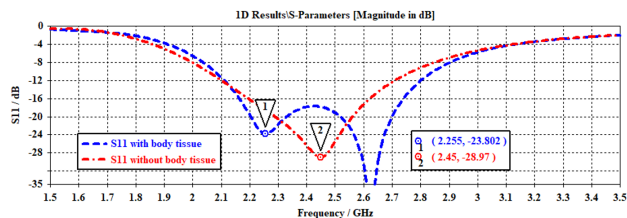


Fig.4: Reflection coefficients of the proposed PIFA in free space and in proximity of the body.

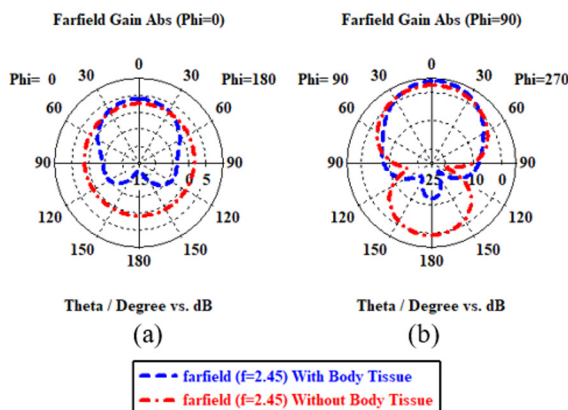


Fig.5: Radiation patterns of proposed PIFA in free space and in proximity of the body at (a) $\Phi=0^\circ$ (b) $\Phi=90^\circ$ cuts.

The next evaluation involves the bending of the proposed antenna around an arm model shown in Figure 6(b). The reflection coefficients of the bent antenna are depicted in Figures 7. It can be seen that the changes in the radius of the arm did not significantly shift antenna resonant frequency. However, a decrease in the antenna bandwidth is seen when it is bent around a smaller arm radius. The antenna performance in flat condition and bending radii of 67.5 mm and 40.5 mm, which are close to realistic radii of the arms of a normal adult, are compared. The antenna resonates at 2.35 GHz, with a bandwidth of 750 MHz when bent on a 67.5 mm arm radius, whereas bending the antenna on a 40.5 mm arm radius slightly lowered the resonant frequency to 2.32 GHz with a bandwidth of 650 MHz. The 750 MHz antenna bandwidth is produced in planar condition, as previously observed. The antenna maintains its dual-band characteristic with a 67.5 mm arm radius. This however, is not the case for the 40.5 mm arm radius.

Table 4: Thickness of each layer in the multilayered human arm model [33].

Layer	Air Gap	Skin	Fat	Muscle	Bone
Thickness (mm)	15	2	10	28	12.5

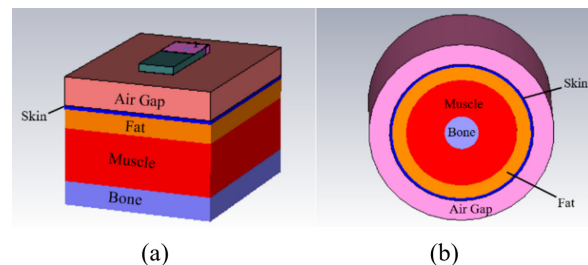


Fig.6: 3D view of two types of phantom models: (a) Flat (b) Cylindrical Arm.

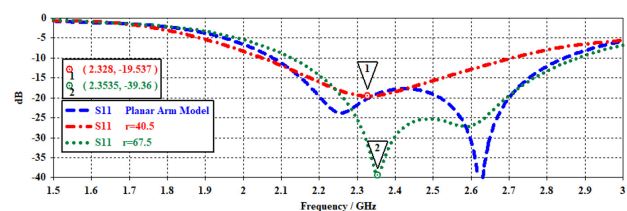


Fig.7: Reflection coefficients of the bent PIFA on the human arm model with radii, $R = 67.5$ mm and 40.5 mm in comparison with the planar condition.

The radiation patterns of the bent antenna are depicted in Figure 8. The maximum gain of the antenna is 3.187 dB and 0.804 dB for larger and smaller arm

radii, respectively. This is mostly due to the degradation of radiation efficiency due to the absorption of electromagnetic power in the lossy body tissues beneath the antenna. Generally, the bigger the arm radius is, the better the antenna performance is.

A comparison between the reflection coefficients of the antenna in flat and bent states are also assessed in free space. This is presented in Figure 9. Based on the comparison with the previous evaluation on the human tissue model in Figure 8, there exists inconsistencies in terms of resonant frequencies between these two cases. Despite this, the changes in gain are clearer, as observed in Figure 10. When bent around the arm model with a 67.5 mm radius, the antenna resonates with a bandwidth of about 730 MHz, centered at 2.54 GHz with a gain of 2.465 dB. For the bending using 40.5 mm of radius, the bandwidth and resonant frequency are 690 MHz and 2.3 GHz, respectively, with a gain of about 2.389 dB. It is clear from these results that antenna gain decreases with the reduction in the bending radii.

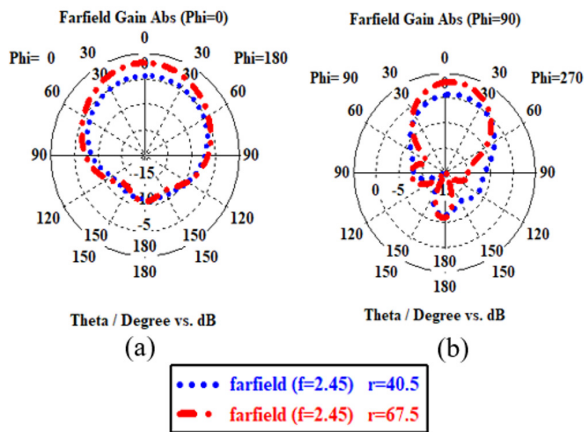


Fig.8: Radiation patterns of the bent PIFA on the human arm model with radii of 67.5mm and 40.5mm at: a) $\Phi=0^\circ$ b) $\Phi=90^\circ$ cut.

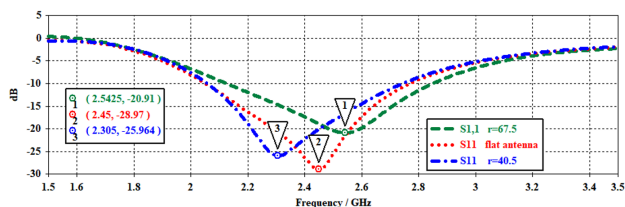


Fig.9: Reflection coefficients of the planar and bent PIFA in free space (without the human arm model).

Next, SAR levels for the bent PIFAs are assessed. The antenna with an input power of 250 mW in the simulations produced a SAR level of 1.97 W/kg, as seen in Figure 11(a). This does not surpass the limitations set by well-known standards such as ICNIRP, which is 2W/kg averaged over 10g of tissues. More-

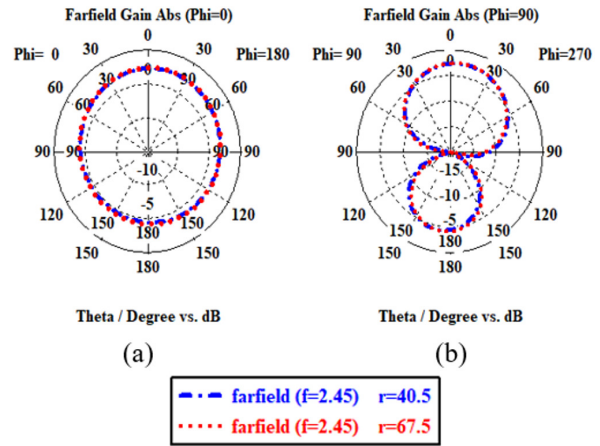


Fig.10: Radiation patterns of bent PIFA in free space with radii of 67.5mm and 40.5mm at: a) $\Phi=0^\circ$ b) $\Phi=90^\circ$ cut.

over, in the 2.43 GHz band, the input power threshold set by FCC, which is limited to 1 W, is also met when using an input power of 250mW. In [27], for the slotted PIFA (SPIFA) located at a distance of 10 mm from the human body in a flat situation and using an input power of 100 mW at 2.45 GHz, measured SAR is about 0.5 W/kg. Similarly, the simulated SAR for the proposed PIFA is 0.807 W/kg when evaluated under the same condition, indicating a reasonable agreement. The small disagreement is due to the difference in the evaluation method in this work, which is conducted in bent condition, while the SAR evaluation in [27] was conducted in planar condition.

6. EFFECT OF HUMIDITY ON ANTENNA PERFORMANCE

In general, textile antenna performance will potentially be affected by humidity or moisture. The high permittivity of water ($\epsilon_r=78$ at 2.45 GHz and 25°C), may result in a raise in a substrate permittivity if it penetrates into that substrate. To evaluate the moisture impact on the antenna performance, simulations using different relative permittivities are performed. In these simulations, other characteristics are presumed unaltered. The initial relative permittivity of this substrate is $\epsilon_r = 1.45$. Figure 12 shows that the resonant frequency shifts towards the lower frequencies as the relative permittivity increases. On the other hand, as the permittivity increases, the $-S_{11}$ is gradually degraded to above -10 dB around $\epsilon_r=2$. These observations are in good agreement with the experimental moisture impact assessments conducted in [25]. Therefore, the impact of humidity on the dielectric loss tangent of textile materials can be further investigated in this way to model this effect in a more precise manner.

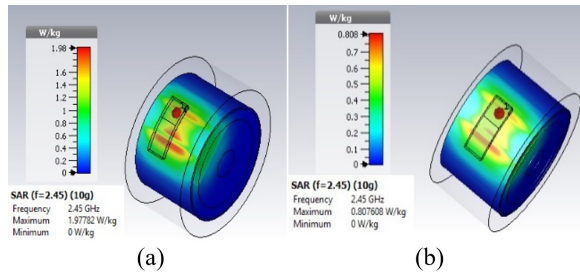


Fig.11: Simulated SAR of the PIFA in bent condition with (a) Input Power=250mW (b) Input Power=100mW.

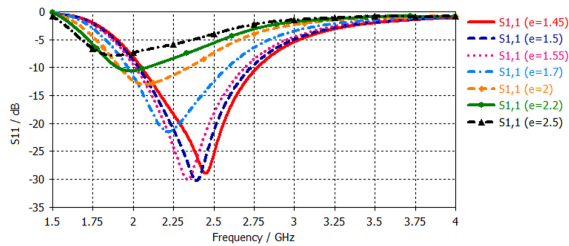


Fig.12: Effect of Permittivity Change (Humidity) on Reflection Coefficient of PIFA.

7. FABRICATION AND MEASUREMENTS

To fabricate this antenna, felt is selected as the substrate, whereas a conductive textile, Aaronia-shield is used as the conductive components – its radiator, shorting wall and ground plane. It is lightweight (about 34g/m^2), with low surface resistance (lower than $0.1\Omega/\text{sq}$) and thus satisfactory surface conductivity. The dimensions of this PIFA is summarized in Table 3. The conductive textiles and substrate are sewn together for mechanical strength, whereas an SMA connector is soldered to the ground plane for galvanic connection. A prototype of the fabricated PIFA is shown in Figure 13.

The simulated and measured reflection coefficients are compared in Figure 14. The antenna operation is centered at 2.5 GHz with a wide 750 MHz of bandwidth, extending from 2.25 GHz to 3 GHz. Meanwhile, the antenna radiation patterns illustrated in Figure 15 indicated a larger discrepancy between simulations and measurements. This is due to the slightly damaged substrate during the soldering process and inaccurate electrical properties of the substrate (permittivity and loss tangent). These properties have been obtained from [9], but are found to be different in practice. Moreover, the sewing process also added more dimensional inaccuracies, which in turn affected the measurement results. The antenna performance on the front and the back of the human body are also measured. These results are similar to the antenna performance when placed on an arm. The antenna placement in these two positions are shown in Figure 16.

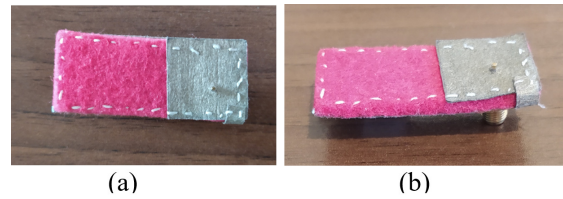


Fig.13: (a) Top (b) Front view of the PIFA Prototype.

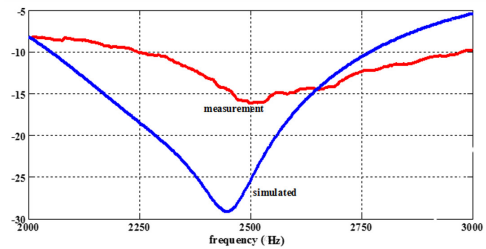


Fig.14: Simulated and measured reflection coefficients of the proposed PIFA.

8. WIRELESS LINK EVALUATION

Being flexible, low in dielectric permittivity, and thus showing low surface wave losses, textiles hold vast potential for IoT applications, especially in wireless-based health monitoring and reporting systems [34]. The operation frequency within the industrial, scientific, and medical (ISM) band overlaps with Bluetooth Low Energy (BLE) standard. This makes the proposed antenna, which operates from 2.25 GHz to about 3 GHz with less than -10 dB of reflection coefficient, suitable for BLE applications.

As the final validation, a single-chip radio transceiver module (nRF24L01 from Nordic Semiconductor) which operates in the 2.4 GHz ISM band was used in this work. This transceiver contains a fully

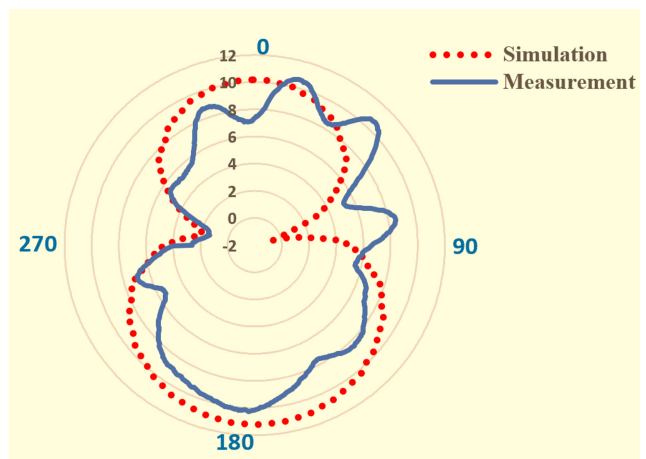


Fig.15: Simulated and measured radiation patterns of the PIFA.

integrated frequency synthesizer, a crystal oscillator, a demodulator, a power amplifier, a modulator, and an Enhanced ShockBurst™ protocol engine. Using an SPI interface, the frequency channels, output power, and protocol setup are easily programmable. Current consumption in RX mode, at an output power of -6dBm is only 9.0mA, which is very low. Built-in Power Down and Standby modes enables power saving realizable [35]. The nominal range of this transceiver is 1800m. Health data using a series of small integrated heartbeat rate sensors, thermal sensors and accelerometers can be collected using this module and communicated to the indoor access point situated remotely.



Fig.16: Placement of the antenna in front and the backside of the human body.

Real-time test data is collected using a laptop computer via a converter board, which connects the USB port of the RF and antenna system to the computer. The prototyped PIFA is then attached to this USB converter board and the NRF24L01 module, as depicted in Figure 17. On the other hand, the remotely located base station (in the form of a laptop) is connected with a monopole antenna, as illustrated in Figure 18. To evaluate the wireless link quality, the wearable system is worn on a human volunteer and set to transmit simple repeated bits in an indoor laboratory environment. This volunteer then gradually moves away from the base station while this assessment continues until the wireless link connection between two nodes is completely disconnected. The wireless link quality of the wearable system with the PIFA is then compared with a simple monopole when worn on the body. It is seen that the link quality for the system using both types of antennas is very similar. The next test moves the base station away from a static wearable node with the proposed PIFA on the body and evaluating the wireless link quality. Due to the severe multipath of the indoor environment, the connectivity range of the link is limited to around 100 meters. The communication between the base station to the on-body wearable system is also illustrated in Figure 18. The ultimate goal of this research is to be able to fully integrate the antenna with the wearable sensors module to track human health, which is aimed to be prototyped in the near future.

9. CONCLUSION

The antenna and RF design and implementation challenges of a body-worn system have been outlined



Fig.17: Wearable textile PIFA with a NRF24L01 and a driver board for wireless link evaluation.

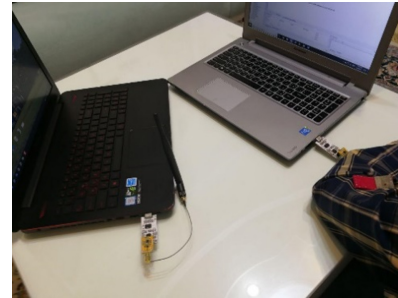


Fig.18: Base station (laptop) and the prototyped PIFA for the wireless link evaluation .

and discussed in this work. To demonstrate the challenging aspects, a Planar Inverted-F antenna was designed using textiles. The proposed antenna is mainly aimed at health monitoring purposes. It can also be used for other applications, including, but not limited to, rescue applications (for example, in firefighters' jacket), security services, sleepwalking accident prevention, sports, and entertainment. For instance, athletes can use this antenna to collect data from different on-body sensors for further investigations [36], [37]. The design process and method of estimating the initial dimensions of this PIFA are first presented, followed by its assessment in flat and bent situations, both on-body and in free space. To guarantee the safety level of the antenna operation on body, the specific absorption rate of this antenna is simulated when placed in the proximity of two types of human arm phantoms, a three-layered rectangular body tissue model, and a three-layered cylindrical human arm model. To assess the severity of the bending on the antenna performance, the antenna is bent over two radii, 40.5 and 67.5 mm, using an arm model. Besides bending, the antenna was also evaluated with different substrate humidity levels, performed by changing its electrical property while assessing the reflection coefficient. Simulation and measurement results of the optimized antenna is then compared in terms of reflection coefficients and radiation patterns. Finally, the proposed antenna is integrated with a nRF24L01 wireless module to evaluate its indoor performance when worn on a human volunteer. Comparison of the proposed PIFA with a simple monopole antenna indicated similar and acceptable performance.

The reported empirical results in this work indicated several limitations that could be addressed in

future research. First, the soldering process is one of the challenges of such works, and it is recommended to be replaced by other alternatives. Second, the sewing process also added more dimensional inaccuracies, for example, compression of the substrate, which in turn affected the measurement results. These physical changes could be avoided by means of special glues; which precise impact must be investigated further in future works. Third, in simulations, it is assumed that the electrical properties of the selected substrate (permittivity and loss tangent) are similar to those of the previously reported works [9] but are found to be different in practice. Fourth, to evaluate the effects of humidity on the antenna performance, the study focused on the variation of relative permittivity and assumed a constant characteristics of the other antenna parameters for the sake of simplicity. In reality, other textile characteristics such as loss tangent may be further affected by humidity.

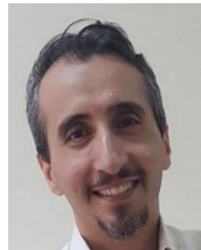
References

- [1] T. N. Gia et al., "Energy efficient wearable sensor node for IoT-based fall detection systems," *Microprocess. Microsyst.*, vol. 56, pp. 34–46, Feb. 2018.
- [2] P. Asghari, A. M. Rahmani, and H. H. S. Javadi, "Internet of things applications: A systematic review," *Computer Networks*, vol. 148, pp. 241 – 261, 2019.
- [3] P. J. Soh, G. A. Vandenbosch, M. Mercuri, and D. M.-P. Schreurs, "Wearable Wireless Health Monitoring: Current Developments, Challenges, and Future Trends," in *IEEE Microwave Magazine*, vol. 16, no. 4, pp. 55-70, May 2015.
- [4] J. Roh, Y. Chi, J. Lee, Y. Tak, S. Nam and T. J. Kang, "Embroidered Wearable Multiresonant Folded Dipole Antenna for FM Reception," in *IEEE Antennas and Wireless Propagation Letters*, vol. 9, pp. 803-806, 2010.
- [5] Rahim, H. A., F. Malek, I. Adam, S. Ahmad, N. B. Hashim, and P. S. Hall, "Design and simulation of a wearable textile monopole antenna for body centric wireless communications," *PIERS Proceedings*, 1381–1384, Moscow, Russia, Aug. 19–23, 2012.
- [6] P. J. Soh, G. A. E. Vandenbosch, S. L. Ooi and N. H. M. Rais, "Design of a Broadband All-Textile Slotted PIFA," in *IEEE Transactions on Antennas and Propagation*, vol. 60, No. 1, pp. 379-384, Jan. 2012.
- [7] S. I. Kwak, D. U. Sim, J. H. Kwon, and Y. J. Yoon, "Design of PIFA with metamaterials for body-SAR reduction in wearable applications," *IEEE Transactions on Electromagnetic Compatibility*, vol. 59, no. 1, pp. 297–300, 2017.
- [8] C. Hertleer, A. Tronquo, H. Rogier, and L. Van Langenhove, "The use of textile materials to design wearable microstrip patch antennas," *Textile Research Journal*, vol. 78, no. 8, pp.651–658, August 2008.
- [9] Soh, P. J., G. A. E. Vandenbosch, S. L. Ooi, and H. M. R. Nurul, "Characterization of a plain broadband textile PIFA," *Radioengineering*, vol. 20, no. 4, pp. 718-725, 2011.
- [10] A. e. a. Yadav, "Wireless Body Area Networks: UWB Wearable Textile Antenna for Telemedicine and Mobile Health Systems," *Micromachines* , 2020.
- [11] A. Sabban, "Wideband Wearable Antennas for 5G, IoT, and Medical Applications," *Advanced Radio Frequency Antennas for Modern Communication and Medical Systems*, IntechOpen, 2020.
- [12] S. Yan, P. J. Soh and G. A. E. Vandenbosch, "Wearable Dual-Band Magneto-Electric Dipole Antenna for WBAN/WLAN Applications," in *IEEE Transactions on Antennas and Propagation*, vol. 63, no. 9, pp.4165-4169, Sep. 2015.
- [13] M. A. A. Majid, M. K. A. Rahim, N. A. Murad and M. H. Mokhtar, "Fully textile slot antenna with curvature analysis," in *2014 IEEE Asia-Pacific Conference on Applied Electromagnetics (APACE)*, pp. 163-166, 2014.
- [14] Hertleer, C.; Rogier, H.; Van Langenhove, L. "A Textile Antenna for Protective Clothing," in *Proceedings of the 2007 IET Seminar on Antennas and Propagation for Body-Centric Wireless Communications*, London, UK, pp. 44–46, 24–24 April 2007.
- [15] B. Ivsic, D. Bonafacic, and J. Bartolic, "Considerations on embroidered textile antennas for wearable applications," *IEEE Antennas Wireless Propag. Lett.*, vol. 12, pp. 1708–1711, Dec. 2013.
- [16] S. Yan, P. J. Soh, and G. A. E. Vandenbosch, "Low-profile dual-band textile antenna with artificial magnetic conductor plane," *IEEE Transactions on Antennas and Propagation*, vol. 62, no. 12, pp. 6487-6490, Dec. 2014.
- [17] Y. Li, Z. Lu, and L. Yang, "CPW-fed slot antenna for medical wearable applications," *IEEE Access*, vol. 7, pp. 42107–42112, 2019.
- [18] S. J. Chen, D. C. Ranasinghe, and C. Fumeaux, "A robust snap-on button solution for reconfigurable wearable textile antennas," *IEEE Trans. Antennas Propag.*, vol. 66, no. 9, pp. 4541–4551, Sep. 2018.
- [19] S. Yan and G. A. E. Vandenbosch, "Radiation pattern-reconfigurable wearable antenna based on metamaterial structure," *IEEE Antennas Wireless Propag. Lett.*, vol. 15, pp. 1715–1718, 2016.
- [20] C.-H. Lin and K. Ito, "A Compact DualMode Wearable Antenna for Body-Centric Wireless Communications," *Electronics*, vol 3, pp. 398-408, Jul. 2014.
- [21] A. Y. I. Ashyap et al., "Compact and low-profile textile EBG-based antenna for wearable medical

- applications,” in *IEEE Antennas and Wireless Propagation Letters*, vol. 16, pp. 2550–2553, 2017.
- [22] R. Salvado, C. Loss, R. Gonçalves, and P. Pinho, “Textile Materials for the Design of Wearable Antennas: A Survey,” *Sensors*, vol. 12, no. 11, pp. 15841–15857, 2012.
- [23] S. Bashir, “Design and synthesis of non-uniform high impedance surface based wearable antennas,” *PhD. Dissertation, Dep. Electronics and Electrical Eng., Loughborough Univ., Leicestershire, UK*, 2009.
- [24] C. Loss, R. Gonçalves, C. Lopes, P. Pinho, and R. Salvado, “Smart coat with a fully-embedded textile antenna for IoT applications,” *Sensors*, vol. 16, no. 6, p. 938, 2016.
- [25] C. Hertleer, A. Van Laere, H. Rogier, and L. Van Langenhove, “Influence of relative humidity on textile antenna performance,” *Textile Res. J.*, vol. 80, no. 2, pp. 177–183, Jan. 2010.
- [26] P. J. Soh, G. a E. Vandenbosch, F. H. Wee, M. Zoinol, A. Abdul, and P. Campus, “Bending Investigation of Broadband Wearable All-Textile Antennas,” *Telecommunication Engineering Dept., Faculty of Electronics and Computer Engineering, Universiti*, vol. 7, no. 5, pp. 91–94, 2013.
- [27] P. J. Soh, G. A. E. Vandenbosch, F. H. Wee, A. van den Bosch, M. Martinez-Vazquez, and D. Schreurs, “Specific Absorption Rate (SAR) Evaluation of Textile Antennas,” *IEEE Antennas and Propagation Magazine*, vol. 57, No. 3, pp. 229–240, June 2015.
- [28] Azeez, Hemin Ismael, Hung-Chi Yang, and Wen-Shan Chen, “Wearable Triband E-Shaped Dipole Antenna with Low SAR for IoT Applications,” *Electronics*, vol. 8, no. 6, pp. 665, 2019.
- [29] S. Sankaralingam, et al., “Performance of Electro-Textile Wearable Circular Patch Antennas in the Vicinity of Human Body at 2.45 GHz,” *Procedia Engineering* vol. 64, pp. 179–184, 2013
- [30] A. Sabban, “Small New Wearable Antennas for IOT, Medical and Sport Applications,” *2019 13th European Conference on Antennas and Propagation (EuCAP)*, pp. 1–5, 2019.
- [31] H. Lee and J. Choi, “A polarization reconfigurable textile patch antenna for wearable IoT applications,” *2017 International Symposium on Antennas and Propagation (ISAP)*, pp.1–2, 2017.
- [32] H. T. Chattha, H. Yi, Z. Xu, and L. Yang, “An empirical equation for predicting the resonant frequency of planar inverted-F antennas,” in *IEEE Antennas and Wireless Propagation Letters*, vol. 8, pp.856–860, 2009.
- [33] H. Vladimír, “Planar antenna in proximity of human body models,” *2013 7th European Conference on Antennas and Propagation (EuCAP)*, pp. 3309–3311, 2013.
- [34] N. F. M. Aun, P. J. Soh, A. A. Al-Hadi, M. F. Jamlos, G. A. E. Vandenbosch, and D. Schreurs, “Revolutionizing wearables for 5G: 5G technologies: Recent developments and future perspectives for wearable devices and antennas,” in *IEEE Microwave Magazine*, vol. 18, no. 3, pp.108–124, May 2017.
- [35] Nordic Semiconductor, “nRF24L01 Single Chip 2.4GHz Transceiver PRELIMINARY PRODUCE SPECIFICATION,” 7075 datasheet, March. 2006.
- [36] J. Trajkovikj, “Robust Wearable UHF Antennas for Security Applications,” (2015).
- [37] K. Damkliang, J. Andritsch, K. Khamkom and N. Thongthep, “A System for Sleepwalking Accident Prevention Utilizing the Remote Sensor of Wearable Device,” *ECTI Transactions on Computer and Information Technology (ECTI-CIT)13*, no.2, pp. 160–169, 2019



Azadeh Ahmadihaji is a Research Assistant in K.N.Toosi University of Technology. She received the bachelor's degree in Electrical engineering, electronics, and master's degree in Telecommunication Engineering from the Bobol Noshirvani University and K.N.Toosi University of Technology in 2014 and 2017, respectively. She has also work experience as a Network Analyzer and Optimization specialist in Telco Industry. Her research interests include wireless sensors, antennas, Telecommunication Networks, IoT, signal processing, and electromagnetics in health.



Hadi Aliakbarian (SM'15) is an Assistant Professor in K.N.Toosi University of Technology in Iran since 2013. He received the B.S and M.S degrees in Electrical and Telecommunication Engineering from the University of Tehran in 2002 and 2005, and the Ph.D degree in Electrical Engineering from the Katholieke Universiteit Leuven (KU Leuven) in 2013. He worked for the microwave laboratory and the Center of Excellence on Applied Electromagnetics at the University of Tehran as an Associated Researcher from 2005 to 2007. He currently leads Wireless Terminal Measurements lab (WiTeM) in K.N.Toosi University of Technology. His research interests include different aspects of antennas, propagation, electromagnetic compatibility and electromagnetics in health and agriculture.



Nordiana Mohamad Saaid was born in Johor, Malaysia. She received the bachelor's degree in Electronics and Communication Engineering from Leeds University, United Kingdom and master's degrees in Telecommunications Engineering from RMIT University, Australia in 2003 and 2007, respectively. She is currently a lecturer in Universiti Malaysia Perlis (UNIMAP) since 2007. She is a member of the Advanced Communication Engineering (ACE) Research Centre in UNIMAP. Her area of interest in research are wearable antennas; on-body communication; GNSS antennas and microwave filters.



Ping Jack Soh received the bachelor and master's degrees from Universiti Teknologi Malaysia, and the PhD degree from KU Leuven, Belgium. He is currently an Associate Professor in the Centre for Wireless Communications (CWC), University of Oulu, Finland. He started his career as a Test Engineer (2002-2004) and R&D Engineer (2005-2006). He then joined Universiti Malaysia Perlis (UniMAP) as a Lec-

turer (2006-2009) before moving to KU Leuven as a Research Assistant (2009-2013), Postdoctoral Research Fellow (2013-2014) and since 2014, a Research Affiliate with the ESAT-WAVECORE Research Division. He went back to UniMAP as a Senior Lecturer (2014-2017) and an Associate Professor (2017-2021) before moving to Finland. Within UniMAP, he was formerly the Deputy Director of the Centre for Industrial Collaboration (2007-2009), Deputy Dean of the university's Research Management and Innovation Center (RMIC) (2014-2017) and Head of the Advanced Communication Engineering (ACE) Research Centre (2020). He researches in antennas and related technologies; focused on their applications in wearables / body area communication; compact satellites; metasurfaces; 5G/6G communications; MIMO, EM safety and absorption; and wireless techniques for healthcare. He is also an Associate Editor of the International Journal of Numerical Modelling: Electronic Networks, Devices and Fields (Wiley).

Dr. Soh was the recipient of the URSI Young Scientist Award in 2015, the IEEE MTT-S Graduate Fellowship for Medical Applications in 2013 and the IEEE AP-S Doctoral Research Award in 2012. He was also the Second Place Winner of the IEEE Presidents' Change the World Competition in 2013. Three of his (co)authored journals were awarded the IEEE Malaysia AP/MTT/EMC Joint Chapter's Publication Award in 2020, 2019 and 2018, and another two journals were also awarded the CST University Publication Award in 2012 and 2011. He is a Chartered Engineer registered with the UK Engineering Council; a Senior Member of the IEEE, and a Member of the IET and URSI. He also volunteers in the IEEE MTT-S Education Committee.